Geophysical Research Letters

RESEARCH LETTER
10.1029/2024GL112537

Observed Sprite Streamer Growth Rates

H. C. Stenbaek-Nielsen[1], M. G. McHarg[2], and N. Y. Liu[3]

[1]Geophysical Institute, University of Alaska Fairbanks, Fairbanks, AK, USA, [2]Department of Physics and Meteorology, United States Air Force Academy, Colorado Springs, CO, USA, [3]Department of Physics and Astronomy, University of New Hampshire, Durham, NH, USA

Key Points:

- Analysis of 165 sprite streamers, imaged at ~100,000 frames per second, verifies the initial exponential growth predicted by theory
- The growth rate is independent of altitude/density; average growth rate increases from C-sprites to Carrots to Jellyfish sprites
- High-speed imaging can provide streamer growth rates and, with a model, the electric field driving the streamers may be derived

Correspondence to:
H. C. Stenbaek-Nielsen,
hcnielsen@alaska.edu

Citation:
Stenbaek-Nielsen, H. C., McHarg, M. G., & Liu, N. Y. (2025). Observed sprite streamer growth rates. *Geophysical Research Letters*, *52*, e2024GL112537. https://doi.org/10.1029/2024GL112537

Received 13 SEP 2024
Accepted 7 DEC 2024

Abstract Sprites have been recorded at ~100,000 frames per second. One hundred and sixty five essentially vertically propagating streamers, 110 downward and 55 upward, have been selected for analysis. The initial velocity increase is exponential as predicted by theory. Growth rates could be determined for 76 downward and 46 upward propagating streamers, and, in individual streamers, they are independent of altitude. The average growth rate increases from 1.6 10^3 in C-sprites, to 2.6 10^3 in carrots, to 8.4 10^3/s in jellyfish sprites. With a streamer model the driving electric field can be derived. Evaluating the field at 70 km altitude, we find fields of 98 (0.45 E_k), 121 (0.56 E_k), and 188 (0.87 E_k) V/m for the 3 sprite types, indicating that jellyfish sprites are the most energetic. High-speed imaging can provide streamer growth rates and combined with a streamer model, the electric fields associated with various sprite features can be investigated.

Plain Language Summary Sprites are electrical discharges in the atmosphere at ~50–90 km altitude caused by low altitude lightning strikes moving electric charges from the clouds to the ground. In a sprite's early phase so-called streamers are observed moving rapidly first downwards and, in some also upwards from altitudes typically in the 70–80 km range. Streamer are small, ~100 m, but very bright ionization fronts moving at velocities around 10,000 km/s. Because of their large velocity high-speed cameras are needed to provide images for analysis. We have recorded sprites at ~100,000 frames per second and we present here an analysis of 165 sprite streamers. Our analysis shows that the streamers indeed accelerate according to the equations predicted by theory. The observed accelerations vary widely and also depend on the type of sprite discharge. This presumably reflects the ambient electric fields which may be derived using suitable modeling. The data presented show that high-speed imaging offers an easy way to derive the ambient electric field driving the streamers, which can then be used to investigate the electric field structures driving the sprites.

1. Introduction

Sprites are electric discharges in the mesosphere observed at altitudes typically between 50 and 90 km. In early video the sprites were seen with red tops and thin blue tendrils reaching down into the lower atmosphere (Sentman et al., 1995; Wescott et al., 1995). When video recordings with higher frame rates became available (Stanley et al., 1999; Stenbaek-Nielsen et al., 2000), it was clear that the tendrils actually are the trails of smaller, bright streamer heads propagating down (review by Stenbaek-Nielsen et al., 2013). Such streamers are well known in electrical discharges (Nijdam et al., 2020; V. P. Pasko, 2006). Reviews of both theoretical and experimental optical work including the many categories of sprites defined by observations have been presented by V. P. Pasko (2010); Pasko et al. (2012); Bor (2013): Stenbaek-Nielsen et al. (2013); and Liu et al., 2015. Streamer models (Kosar et al., 2012; Kulikovsky, 1997; Liu et al., 2009) predict that in a constant electric field the velocity will increase exponentially, and that the growth rate will increase with increasing electric field. We present here observations confirming this prediction.

We analyzed 165 streamers propagating up and down several 10s of km from onset to fade. The streamer path typically starts with a section in which the velocity and brightness increases rapidly. Later, the velocity slows and, eventually, the streamer fades. The analysis covers the initial section with increasing velocity only. The velocity, and subsequently the growth rate, is derived from the change in altitude observed over a sequence of images. The growth rate derivation is relatively simple, and coupled with a streamer model it can be used to map the ambient electric field in the vicinity of the streamers.

2. Data and Streamer Selection

The high speed sprite recordings were made on the nights of June 2 and 3, 2019, from the Langmuir Laboratory for Atmospheric Research near Socorro, New Mexico. The Observatory is at an altitude of 3.3 km at 33.975° N, 107.181° W. The sprites were clustered over an intense thunderstorm complex in western Texas due east of the observing site. On the two nights of observations, the sprite clusters were 690 and 465 km, respectively, from the observatory. A map giving the locations was presented by Contreras-Vidal et al. (2021)—their Figure 2.

The images were recorded using a Phantom V2611 camera (12 bit images) with a VS-1845HS intensifier (1 μs decay phosphor). At ∼100,000 fps the hardware limits the size of the images. On 2 June 2019 we used an 85 mm lens giving a 9.9° × 6.3° image (512 × 320 pixels) which typically will contain the entire sprite. The pixel resolution at the distance of the sprites is ∼250 m. On 3 June 2019 we used a 300 mm lens for better spatial resolution, ∼45 m pixel resolution at the sprites. The image size was varied during the night, but most recordings used a 1.4° × 2.8° image (256 × 512 pixels). While the smaller field limits the sprite coverage the 512 pixel height gives good altitude coverage, a feature very valuable for the study reported here. Co-mounted with the Phantom camera was a low light-level video camera (Watec 902H) to provide scene awareness and to record the star background critical for accurate pointing information. All images have GPS time.

The altitude of the streamers was calculated from look angles (azimuth and elevation derived from the star background) and range to the sprite. For some sprites observed on 3 June 2019 the range could be triangulated using images recorded by T. Ashcroft at Lamy, NM. Otherwise, we used the range to the causal lightning strike as recorded by NLDN or ENTLN. The sprites may not be over the lightning strike (discussion in Stenbaek-Nielsen et al., 2020); a 40 km uncertainty on range will give an altitude uncertainty of 3–4 km (∼half of the atmospheric neutral density scaleheight).

The data set has 53 high-speed Phantom recordings some of which have several sprites, and we identified for the analysis streamers in 41 individual sprites (21 on 2 June 2019, and 20 on 3 June 2019) with onset within the Phantom field of view and with simultaneous Watec images for directional information. In each of the 41 sprites we identified a number of streamers for analysis. We selected dominant downward and upward propagating streamers with onset within, or very near to, the Phantom field of view and which could be followed in many frames until they faded or exited the image field of view. Many streamers split one or more times. In this case we followed only the dominant sub-streamer out of the split. Many of the sprites have a large number of streamers. In one large sprite we counted more than 50 downward propagating streamers. In these sprites, we selected ∼5 representative examples for analysis. Not considered were streamers propagating across the image.

The selection yielded a total of 165 streamers; 110 were downward propagating streamers and 55 upward propagating streamers. Of the 165 streamers 37 were in C-sprites; 105 in Carrots; and 23 in jellyfish sprites. We define jellyfish sprites as large, short duration, sprites with a diffuse upward propagating feature instead of streamers, as described by Pasko et al. (2012). Thus, upward streamers are in carrots only. For each streamer we recorded the pixel location in successive Phantom images, and with direction (azimuth and elevation) and range the altitude can be calculated to provide profiles of altitude versus time.

The pixel location of the streamers in the images was done visually. Various computer routines were tried to get better than one pixel resolution, but they could not be applied consistently across the data, and, more seriously, they resulted in shorter time-series. It would have been desirable to have streamer brightness and diameter, however, to add these parameters significantly complicate the analysis, and we decided to leave that for a later analysis effort.

A typical streamer altitude/time profile starts with a section with increasing velocity. Later, the velocity slows, and eventually, the streamer fades. In upward propagating streamers the fade is often associated with a transition into a diffuse glow that fades exponentially (Stenbaek-Nielsen et al., 2023). For the study presented here we are only looking at the initial section with increasing velocity, which is not present in all 165 streamers in our data set. Some are only getting bright enough for detection well after onset when the velocity is essentially constant, and in very bright sprites the initial phase may not be properly resolved even in recordings at 100,000 fps. Also, the rapid increase in brightness leads to saturation which limits analysis. Nevertheless, analysis of the initial velocity increase was possible for 122 out of the 165 streamers in the data set.

3. Streamer Velocity Analysis

The altitude profiles, h(t), have the streamer altitude as function of time. Corresponding velocity profiles, v (t) = dh(t)/dt, were derived from the slope of the altitude profile, which, for each point in the profiles, is calculated by a least squares fit to a line using 11 altitude points centered on the point. The 11-point fit to derive the velocity profiles appears to be a good compromise. Fewer points result in more noise in the profiles, and more points, while providing visibly smother profiles, will limit the resolution in streamers with rapidly changing velocities as is often observed in bright streamers.

In a constant ambient electric field theory predicts that the initial downward streamer velocity will increase exponentially (Kosar et al., 2012; Kulikovsky, 1997; Liu et al., 2009). Hence, on a log-velocity plot the increase will be linear and the slope is the growth rate. It is worthwhile to note that since we assume a constant range to the streamer, the derived growth rate is essentially independent of the range.

Another way to derive streamer velocities and growth rate is by fitting the altitude profile to an assumed analytic function. With the expected exponential velocity increase the streamer velocity should fit a function of form

$$v(t) = v_0 \exp((t - t_0)\gamma) \quad (1)$$

where γ is the streamer growth rate defined by theory and ultimately tied to the external electric field driving the streamer, and v_0 is the streamer velocity at time t_0.

The streamers selected for analysis propagate essentially vertically. Thus the altitude can be derived from the velocity function by integration:

$$h(t) = h_0 + (v_0/\gamma)(\exp((t - t_0)\gamma) - 1) \quad (2)$$

where h_0 is the streamer altitude at time t_0. The exponential function is overlaid the observed images initially using values from the log-velocity plot. The growth rate and the beginning and end altitudes can then be adjusted for a best "visual fit" or for a least-squares fit between the function altitudes and the observed altitude profile, $h(t)$. In streamers with longer altitude time series the "visual fit" is clearly affected with a change in growth rate of 100/s. This is why we found it important to follow the selected streamers over as large an altitude range as possible.

Velocity growth rates were derived using both analysis methods, and the two methods complement each other well as would be expected. Our streamer data set has 110 profiles for downward and 55 profiles for upward propagating streamers, and we could derive velocity growth rates for 76 and 46 profiles, respectively. In the following we present analysis results for 3 streamers; two downward propagating streamers, one emerging from a dark sky and one emerging from a sprite halo, and the third, an upward propagating streamer. The three streamers are quite representative of the larger data set.

3.1. Downward Streamers

Figure 1 shows a downward propagating streamer recorded at 100,000 fps on 3 June 2019 at 04:45:48 UT in a bright carrot. Most of the activity was outside the 2.9° × 1.8° (42 m pixel resolution) Phantom field of view. The streamer was first detected near 75 km altitude with onset in "dark sky"; no halo was detected. This is not unusual and likely just reflects insufficient camera sensitivity (Liu et al., 2015). The streamer slowly brightened and propagated down. It was followed for 90 frames (0.90 ms) until it exited the field of view at 63 km altitude. At this time the streamer was slowing and fading. The top plots show the altitude profile for the streamer and the streamer velocities. The velocity increases exponentially (linear increase on the log scale plot) over the first 80 points of the profile, and the fitted line gives the growth rate, 2.5 10^3/s. At the bottom is a time series of image sections centered on the streamer with the exponential function overlaid.

Some downward propagating streamers are observed emanating from the bottom of a sprite halo as reported by Cummer et al. (2006); McHarg et al. (2007) and modeled by Liu et al. (2009, 2015) and Luque and Ebert (2009). The streamer velocities are generally higher than for streamers emerging from essentially a dark sky (Figure 1), and they develop significantly faster. Figure 2 shows a downward propagating streamer emerging from the halo at the start of a jellyfish sprite recorded at 98,073 fps on 3 June 2019 at 05:07:18 UT. The Phantom field of view is

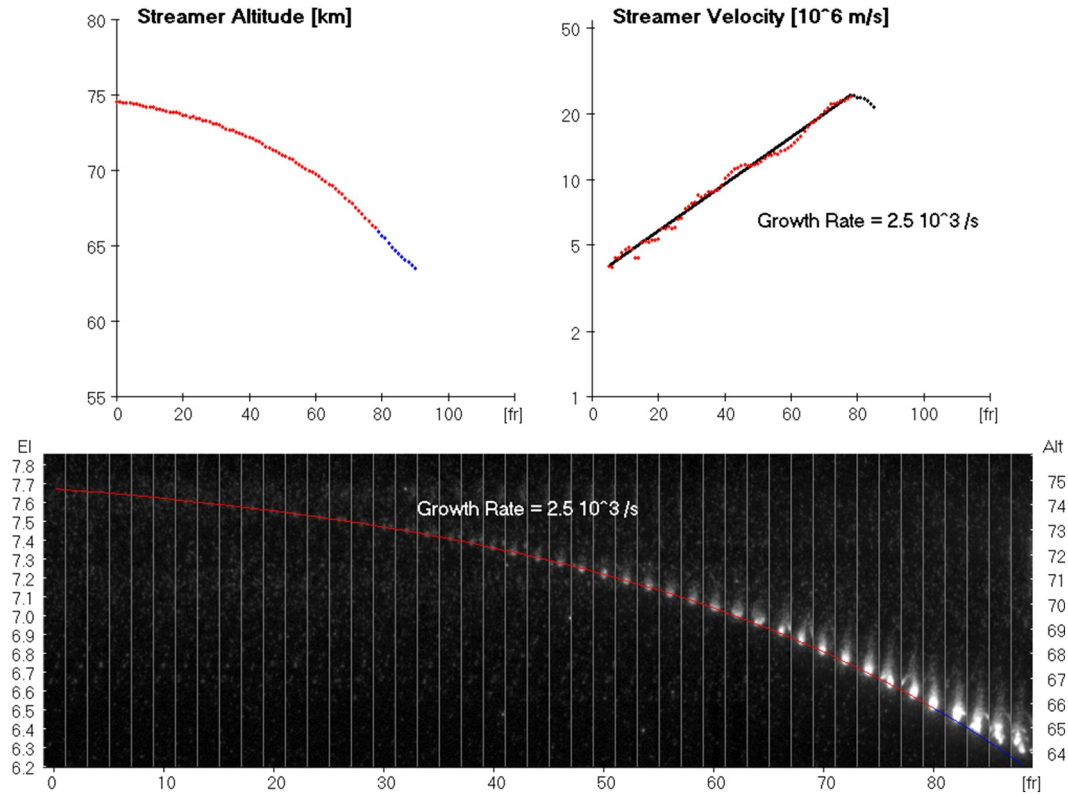

Figure 1. Altitude profile and streamer velocities derived for a downward propagating streamer in a carrot recorded at 100,000 fps on 3 June 2019 at 04:45:48 UT. The velocity increases exponentially over its initial path, frame 0 to 80, and the growth rate, 2.5 10^3/s, appears to be independent of altitude. The data points used for the fit are shown in red. Video at Stenbaek-Nielsen et al. (2024).

1.4° × 2.8° with a pixel resolution of 45 m. The streamer is bright and eventually saturates the imager, but the downward propagation is well defined. The upper left image shows the streamer having just emerged from the structured halo. The box gives the 0.2° × 1.8° image section used to create the image strip time series. The plots are the altitude streamer profile and the velocities derived from the profile.

The streamer is first identifiable at an altitude of 78.5 km. This is frame 0 in the strip image panel. The streamer velocity has an initial rapid increase, followed by a relatively constant velocity section, and then a decrease as the streamer propagates down into the lower, denser atmosphere. We see that in many downward propagating streamers. In this streamer the velocity increase is over 12 frames only. Our older sprite recordings at ∼10,000 fps would not have resolved this; the streamer would have emerged at maximum velocity (example in Stenbaek-Nielsen et al. (2020)—their Figure 3).

The initial growth rate from the altitude profile is 1.2 10^4/s (top right), and the corresponding exponential function fits the observed streamer motion well (bottom panel). The exponential velocity increase ends near frame 11 in the image strip figure, and a few frames earlier in the profile velocity plot. The difference is an artifact of the 11-point profile section used to calculate the velocity. The downward velocity at frame 0 is 1.5 10^7 m/s increasing to 5.6 10^7 m/s at frame 11. After that the velocity levels off and starts to decrease near frame 25. At streamer onset the downward velocity is similar to that of the descending halo; we see that as well in other sprites with streamer onset in the descending halo.

To allow the reader to evaluate the streamer onset we inserted in the strip figure a small segment of the strip image time series without the exponential. A similar temporal development as shown here, but from a computer model, has been given by Liu et al. (2009)—their Figure 2.

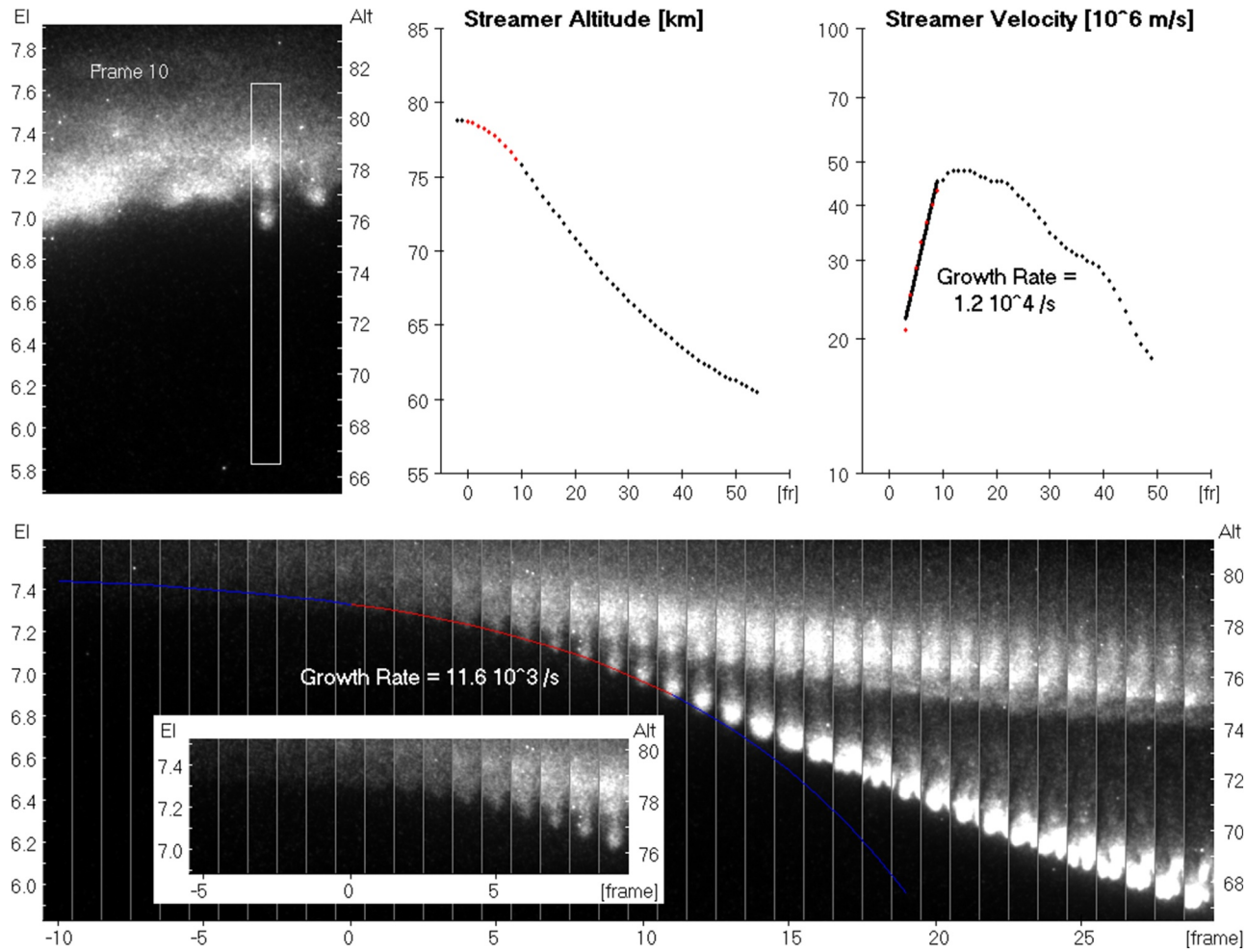

Figure 2. Streamer with onset, frame 0, in the bottom of a bright descending halo. The sprite is a jellyfish recorded at 98,073 fps on 3 June 2019 at 05:07:18 UT. The growth rate is 1.2 10^4/s. After frame 11 the streamer departs from the initial exponential growth. The downward velocity at streamer onset, frame 0, is 1.5 10^7 m/s increasing to 5.6 10^7 m/s at frame 11. The exponential growth rate is based on frames 0 to 11 (points in red). In the bottom panel the exponential function altitude outside the 0–11 image section is shown in blue. Video at Stenbaek-Nielsen et al. (2024).

3.2. Upward Streamer

Figure 3 shows an upward propagating streamer recorded in a carrot sprite on 2 June 2019 at 07:46:35 UT at 100,000 fps. The onset was at 66 km altitude in the top of glow from the initial downward propagating streamer. The streamer was followed for 90 frames (0.90 ms) until the streamer slowed and faded near 90 km altitude. At about 82 km it started to transit from a small discrete streamer to a more diffuse feature. This temporal development is quite typical of many of the 55 upward propagating streamers analyzed. The streamer is one of four isolated streamers in 2 carrots discussed in Stenbaek-Nielsen et al. (2023). The fade of the diffuse streamer head is exponential, and we suggested that the time constant for the fade together with the altitude can provide information about the ambient electron density.

The top plots show the streamer altitude profile and the velocities. The velocity increases exponentially over the first 68 frames with a growth rate of 3.3 10^3/s. The velocity increase near the top relative to the growth rate line is almost certainly not real, but an artifact of the scaled streamer center locations which were done visually. The increase may reflect an expansion of the streamer head as it transits to a more diffuse appearance. As was the case for the downward propagating streamer in Figure 1, the streamer growth rate during the initial phase of the streamer propagation does not change with altitude; no effects from the changing atmospheric density are evident in the derived velocities.

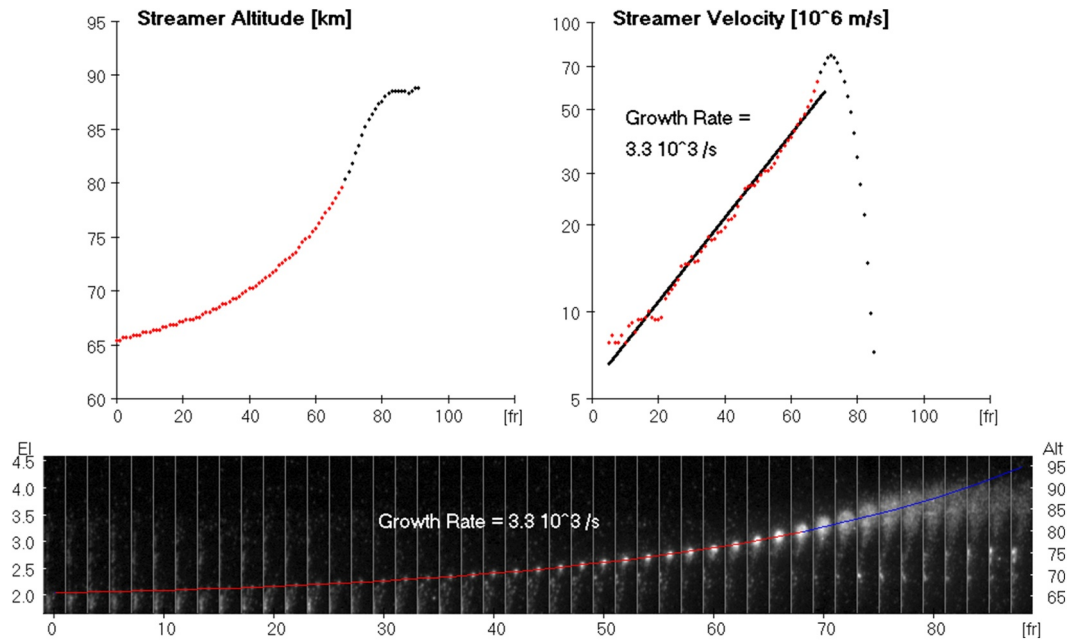

Figure 3. Altitude profile and streamer velocities derived for an upward propagating streamer in a carrot recorded at 100,000 fps on 2 June 2019 at 07:46:35 UT. On the logarithmic velocity plot the increase is linear showing that the increase is exponential. The growth rate, 3.3 10^3/s, is independent of altitude. The section of the streamer profile used to determine the growth rate is shown in red. The function beyond this section (bottom panel) is in blue. Video at Stenbaek-Nielsen et al. (2024).

4. Summary of Growth Rate Analysis

A summary of the streamer growth rate analysis is given in Figure 4. The 2 plots in the top row show histograms of the streamer growth rates, and the bottom 2 plots show the altitude range over which we observe a constant growth rate. The plots to the left are for downward propagating streamers in C-sprites, Carrots, and Jellyfish sprites, and to the right growth rate data for carrots. With our sprite classification definitions only carrots have significant upward propagating streamers; jellyfish have instead of upward propagating streamers an upward propagating diffuse glow. Mean values and standard deviations, STD, for the growth rates in the different sprite classes are given in the top row histogram plots, and the streamers in Figures 1–3, are identified in the bottom row plots.

The distribution of the derived growth rates differs between the sprite classes. The lowest growth rates are in C-sprites followed by carrots with mean values 1,574 and 2,629/s, respectively. In contrast, the growth rates in jellyfish streamers are generally higher with a mean at 8,363/s. The distribution is also much broader; actually, the 12,000–14000 bin includes 2 streamers with growth rates above 14,000/s, the highest being 1.7 10^4/s. The histogram plot for streamers in carrot sprites show upward propagating streamers with generally higher growth rates than downward propagating streamers.

5. Discussion

The analysis presented here shows that sprite streamers after onset grow exponentially confirming predictions by theory (Kosar et al., 2012; Kulikovsky, 1997; Liu et al., 2009). Although not explicitly discussed, the exponential growth is also present in recent simulations by Bouwman et al. (2024). We analyzed 110 altitude profiles for downward and 55 profiles for upward propagating streamers, and we could derive velocity growth rates for 76 and 46 profiles, respectively. The observations show the streamer growth rate to be independent of altitude. Some streamers propagate over altitudes larger than the atmospheric scale height, for example, from onset at 74–66 km (Figure 1) and from 65 to 80 km (Figure 3), but the observed velocity growth rate does not change.

In bright streamers the initial exponential velocity increase is typically short, 10 to 20 frames, and those streamers have higher growth rates. This is clearly evident in Figure 4 where streamers with higher growth rates, in

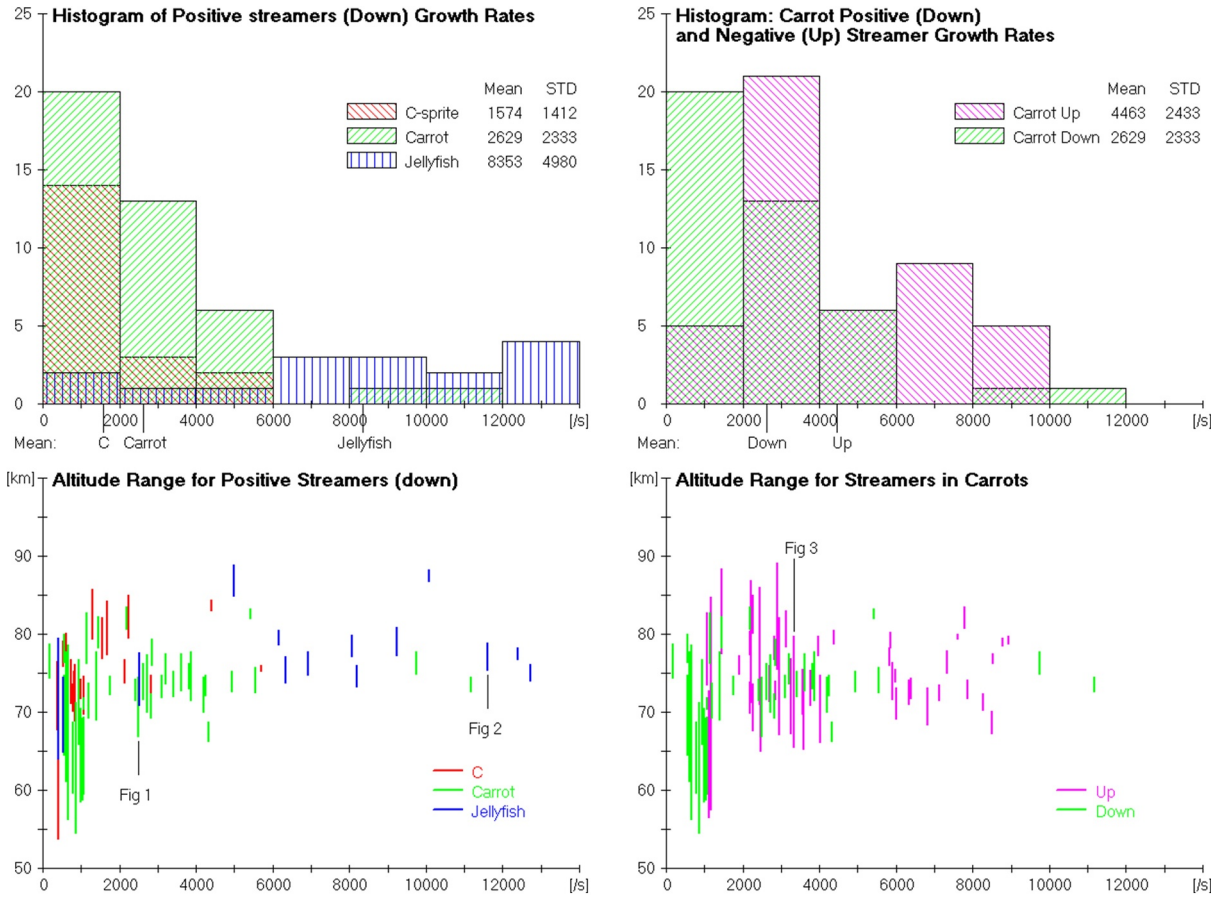

Figure 4. Summary of the streamer growth rate analysis. Top plots show histograms for the downward propagating streamers, and the downward and upward propagating streamers in carrots. Bottom plots show the altitude range with constant growth rate for the streamers analyzed.

particular jellyfish streamers, have altitude ranges less than 5 km. For the streamer in Figure 2 the altitude range is 4 km.

The 76 observed growth rates for downward propagating streamers include 19 for C-sprites, 41 for carrots, and 16 for jellyfish sprites (summary in Figure 4 above). The growth rates vary considerably, but the figure clearly shows the lowest growth rates are in C-sprites and the highest in jellyfish sprites. The analysis also shows the growth rates in upward propagating streamers are generally higher than in the downward propagating carrot streamers. This is much as expected; the only surprise is the much larger growth rates in jellyfish sprites.

The streamers are driven by an external electric field (Liu et al., 2009), and with a suitable streamer model the external field may be derived. Kosar et al. (2012) using a streamer model by N. Liu and Pasko (2004), simulated short streamers at different altitudes. They found that the growth rate scales with air density, and they presented plots from which the external electric field can be derived from streamer growth rate and altitude. The study concentrated on growth rates for electric fields below the local break-down electric field, E_k, however, the N. Liu and Pasko (2004) model itself is valid also for higher fields. We used Kosar et al. (2012) Figure 5a to scale the growth rate to 75 km altitude, and then Figure 5b to give the ambient electric field. The Kosar plots cover a large fraction of the streamers in our data set, but not many of the higher growth rate streamers observed primarily in jellyfish. While the observed growth rate is insensitive to the distance to the sprite, the derived streamer altitude is not, and this must be kept in mind when using the observations to derive the ambient electric fields.

The mean growth rates for streamers in C-sprites, carrots, and jellyfish are 1,574, 2,629, and 8,353/s, respectively. Evaluated at 70 km altitude the model gives 98, 121, 188 V/m, showing the jellyfish sprites are associated with the largest electric fields. As a fraction of the local electric break-down field, E_k, the fields are 0.45, 0.56, and 0.87 E_k. E_k scales with the atmospheric density, and the Kosar model uses a value of 32 kV/cm at ground level.

The streamers in Figures 1 and 3 are covered by the model, but the growth rate for the streamer in Figure 2 is too high. The growth rate in Figure 1 is 2.5 10^3/s between altitudes 74 and 66 km leading to an ambient electric field varying from 82 to 162 V/m or 0.67 to 0.45 E_k. Figure 3 has an upward propagating streamer with a growth rate of 3.3 10^3/s between 66 and 79 km altitude leading to a field varying from 181 to 47 V/m or 0.50 to 0.93 E_k. In both cases the electric field decreases with altitude. The decrease with altitude is a factor of 0.50 (Figure 1) and 0.29 (Figure 3), but the atmospheric density decreases faster, factors of 0.34 and 0.14, over the same two altitude ranges. Thus, the observations show that the lightning field at sprite altitudes decreases slower than the air density confirming the prediction by C.T.R. Wilson (1925).

Our analysis suggests that high-speed imaging can provide streamer growth rates for a majority of streamers observed, and with a streamer model the mesospheric electric field structures in the vicinity, even in spatially complex sprites, can be mapped. Imaging at high speed provides a relatively simple and easy way to derive the electric fields driving the streamers. The fields can then be related to the many and varied observed luminous sprite features to further our understanding of sprite streamer physics.

Data Availability Statement

Videos of the sprites are available at Center of Open Science, OSF (H. C. Stenbaek-Nielsen, 2024).

Acknowledgments
We thank H. Edens, R. Sonnenfeld and C. da Silva for discussions and access to the Langmuir laboratory, and Mr. T. Ashcroft, Lamy, NM, for sprite images from the night of 3 June 2019. M. McHarg was supported by the Air Force Office of Scientific Research and N. Liu by NSF Award AGS-2247153 to the University of New Hampshire.

References

Bor, J. (2013). Optically perceptible characteristics of sprites observed in Central Europe in 2007–2009. *Journal of Atmospheric and Solar-Terrestrial Physics*, *92*(2013), 151–177. https://doi.org/10.1016/j.jastp.2012.10.008

Bouwman, D., Teunissen, J., & Ebert, U. (2024). Macroscopic parameterization of positive streamer heads in air. *Plasma Sources Science and Technology*, *31*(4), 045023. https://doi.org/10.1088/1361-6595/ac64bf

Contreras-Vidal, L., Sonnenfeld, R. G., da Silva, C. L., McHarg, M. G., Jensen, D., Harley, J., et al. (2021). Relationship between sprite current and morphology. *Journal of Geophysical Research: Space Physics*, *126*(3), e2020JA028930. https://doi.org/10.1029/2020JA028930

Cummer, S. A., Jaugey, A. N., Li, J., Lyons, W. A., Nelson, T. E., & Gerken, E. A. (2006). Submillisecond imaging of sprite development and structure. *Geophysical Research Letters*, *33*(4), L04104. https://doi.org/10.1029/2005GL024969

Ebert, U., Nijdam, S., Li, C., Luque, A., Briels, T., & van Veldhuizen, E. (2010). Review of recent results on streamer discharges and discussion of their relevance for sprites and lightning. *Journal of Geophysical Research*, *115*(A7), A00E43. https://doi.org/10.1029/2009JA014867

Kosar, B. C., Liu, N., & Rassoul, H. K. (2012). Luminosity and propagation characteristics of sprite streamers initiated from small ionospheric disturbances at subbreakdown conditions. *Journal of Geophysical Research*, *117*(A8), A08328. https://doi.org/10.1029/2012JA017632

Kulikovsky, A. A. (1997). The mechanism of positive streamer acceleration and expansion in air in a strong external field. *Journal of Physics D: Applied Physics*, *30*(10), 1515–1522. https://doi.org/10.1088/0022-3727/30/10/019

Li, J., & Cummer, S. A. (2009). Measurement of sprite streamer acceleration and deceleration. *Geophysical Research Letters*, *36*(10), L10812. https://doi.org/10.1029/2009GL037581

Liu, N., & Pasko, V. P. (2004). Effects of photoionization on propagation and branching of positive and negative streamers in sprites. *Journal of Geophysical Research*, *109*(A4), A04301. https://doi.org/10.1029/2003JA010064

Liu, N. Y., Dwyer, J. R., Stenbaek-Nielsen, H. C., & McHarg, M. G. (2015). Sprite streamer initiation from natural mesospheric structures. *Nature Communications*, *6*(1), 7540. https://doi.org/10.1038/ncomms8540

Liu, N. Y., Pasko, V. P., Adams, K., Stenbaek-Nielsen, H. C., & McHarg, M. G. (2009). Comparison of acceleration, expansion and brightness of sprite streamers obtained from modeling and high-speed video observations. *Journal of Geophysical Research*, *114*(A3). https://doi.org/10.1029/2008JA013720

Luque, A., & Ebert, U. (2009). Emergence of sprite streamers from screening-ionization waves in the lower ionosphere. *Nature Geoscience*, *2*(11), 757–760. https://doi.org/10.1038/ngeo662

McHarg, M. G., Stenbaek-Nielsen, H. C., & Kammae, T. (2007). Observation of streamer formation in sprites. *Geophysical Research Letters*, *34*(6), L06804. https://doi.org/10.1029/2006GL027854

Niijdam, S., Teunissen, J., & Ebert, U. (2020). The physics of streamer discharge phenomena. *Plasma Sources Science and Technology*, *29*(10), 103001. https://doi.org/10.1088/1361-6595/abaa05

Nudnova, M. M., & Starikovskii, A. Y. (2008). Streamer head structure: Role of ionization and photoionization. *Journal of Physics D: Applied Physics*, *41*(23), 234003. https://doi.org/10.1088/0022-3727/41/23/234003

Pasko, V. P. (2006). Theoretical modeling of sprites and jets. In M. Füllekrug, E. A. Mareev, & M. J. Rycroft (Eds.), *Sprites, Elves and Intense Lightning Discharges* (Vol. 225, pp. 253–311). Springer. NATO Science Series II: Mathematics, Physics and Chemistry. https://doi.org/10.1007/1-4020-4629-4_12

Pasko, V. P. (2010). Recent advances in theory of transient luminous events. *Journal of Geophysical Research*, *115*(A6). https://doi.org/10.1029/2009JA014860

Pasko, V. P., Yair, Y., & Kuo, C.-L. (2012). Lightning related transient luminous events at high altitude in the Earth's atmosphere: Phenomenology, mechanisms and effects. *Space Science Reviews*, *168*(1–4), 475–516. https://doi.org/10.1007/s11214-011-9813-9

Sentman, D. D., Wescott, E. M., Osborne, D. L., Hampton, D. L., & Heavner, M. J. (1995). Preliminary results from the Sprites94 campaign: Red sprites. *Geophysical Research Letters*, *22*(10), 1205–1208. https://doi.org/10.1029/95GL00583

Stanley, M., Krehbiel, P., Brook, M., Moore, C., Rison, W., & Abrahams, B. (1999). High speed video of initial sprite development. *Geophysical Research Letters*, *26*(20), 3201–3204. https://doi.org/10.1029/1999GL010673

Stenbaek-Nielsen, H. C. (2024). Observed sprite streamer growth rates [Dataset]. *OSF*. https://doi.org/10.17605/OSF.IO/nuq9k

Stenbaek-Nielsen, H. C., Kanmae, T., McHarg, M. G., & Haaland, R. (2013). High-speed observations of sprite streamers. *Survey of Geophysics*, *34*(6), 769–795. https://doi.org/10.1007/s10712-013-9224-4

Stenbaek-Nielsen, H. C., Liu, N. Y., McHarg, M. G., & Harley, J. (2023). D region electron density derived from sprite observations. *Geophysical Research Letters*, *50*(2), e2022GL101575. https://doi.org/10.1029/2022GL101575

Stenbaek-Nielsen, H. C., McHarg, M. G., Haaland, R., & Luque, A. (2020). Optical spectra of small-scale sprite features observed at 10,000 fps. *Journal of Geophysical Research: Atmospheres*, *125*(20), e2020JD033170. https://doi.org/10.1029/2020JD033170

Stenbaek-Nielsen, H. C., Moudry, D. R., Wescott, E. M., Sentman, D. D., & Sao Sabbas, F. T. (2000). Sprites and possible mesospheric effects. *Geophysical Research Letters*, *27*(23), 3829–3832. https://doi.org/10.1029/2000GL003827

Wescott, E. M., Sentman, D., Osborne, D., Hampton, D., & Heavner, M. (1995). Preliminary results from the Sprites 94 aircraft campaign: 2. Blue jets. *Geophysical Research Letters*, *22*(10), 1209–1212. https://doi.org/10.1029/95GL00582

Wilson, C. T. R. (1925). The electric field of a thundercloud and some of its effects. *Proceedings of the Physical Society of London*, *37*(1), 32D–37D. https://doi.org/10.1088/1478-7814/37/1/314